Process Safety and Environmental Protection 210 (2026) 108687

Contents lists available at ScienceDirect

Process Safety and Environmental Protection

journal homepage: www.journals.elsevier.com/process-safety-and-environmental-protection

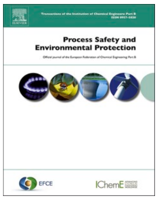

Flash point behavior of multicomponent terpene mixtures: An experimental and modeling study

Sérgio M. Vilas-Boas [a,*,1], Fernanda Sossai Altoé [b,1], Eduardo de Souza Esperança [b], Filipe Hobi Bordón Sosa [c], Débora Costa do Nascimento [b], Antonio M. Barbosa Neto [d], Mariana Conceição da Costa [b,*]

[a] CRETUS, Department of Chemical Engineering, Universidade de Santiago de Compostela, Santiago de Compostela, E-15782, Spain
[b] School of Chemical Engineering (FEQ), Universidade Estadual de Campinas (UNICAMP), Campinas, 13083-852, Brazil
[c] CICECO – Aveiro Institute of Materials, Department of Chemistry, University of Aveiro, Aveiro, 3810-193, Portugal
[d] ThermoPhase, Department of Petroleum Engineering, Santa Catarina State University, Balneário Camboriú, 88336-275, Brazil

ARTICLE INFO

Keywords:
Flash point
Essential Oils
Le Chatelier's rule
Liaw-UNIFAC
COSMO-RS
Process Safety

ABSTRACT

The flash point (FP) is a critical property for assessing fire and explosion hazards of flammable liquids. However, reliable FP data for terpene-rich mixtures are scarce, despite their relevance as the major constituents of commercial essential oils. This work provides a comprehensive investigation of the FP behavior of four naturally abundant monoterpenoids—*p*-cymene, linalool, carvacrol, and eugenol—and their binary and ternary mixtures. Experimental measurements were performed using the ASTM D6450 closed-cup procedure, revealing a quasi-linear relationship between the FP and the normal boiling point for the pure compounds. The mixtures, however, exhibited complex structure-property relationships, where specific intermolecular interactions play a key role in the FP behavior. To complement the experimental studies, the predictive capabilities of the Liaw-UNIFAC and COSMO-RS models were benchmarked against the ideal approach for the mixtures. COSMO-RS provided the best overall representation, with a global RMSE of 0.9 K. The Liaw-UNIFAC (global RMSE = 2.9 K) outperformed the ideal approach (RMSE = 3.6 K) in six of the ten mixtures studied, highlighting that its performance is highly system-dependent. This work delivers crucial experimental data and validates a modeling framework for assessing the FP of multicomponent monoterpene mixtures, providing valuable insights for process safety and fire risk assessment in the EO industry.

1. Introduction

Essential oils (EOs) are predominantly hydrophobic, volatile liquid mixtures obtained from aromatic plant materials, typically by distillation processes (Ivanova et al., 2025). These naturally derived mixtures typically exhibit characteristic aromas and interesting biological and pharmacological properties, finding applications in numerous fields, including the food, pharmaceutical, and cosmetic industries (Al-Maqtari et al., 2022; Carvalho et al., 2016; Cimino et al., 2021; Sharmeen et al., 2021). The economic relevance of the EOs is reflected in their market size, valued at USD 23.74 billion in 2023, with a projected growth of 7.5% from 2024 to 2030 (Baser and Bonello, 2025). From a chemical perspective, EOs exhibit high diversity, often comprising more than 200 individual components, including terpenes, hydrocarbons, alcohols, aldehydes, acids, esters, ketones, phenols, lactones, and their derivatives (Hanif et al., 2019). Despite the notable complexity, monoterpenes and their oxygenated derivatives—the monoterpenoids—typically represent the dominant fraction, frequently accounting for over 50% of the total composition of the EO profile (Yu, 2025; Zielińska-Błajet and Feder-Kubis, 2020).

Monoterpenes and monoterpenoids are characterized by distinct aromas and a wide range of biological and pharmacological properties, such as antioxidant, anti-inflammatory, antifungal, and analgesic activities (Jávega-Cometto et al., 2025). This multifunctionality supports their extensive use as natural ingredients in the fragrance, cosmetic, and food industries (Masyita et al., 2022; Paulino et al., 2022; Zielińska-Błajet and Feder-Kubis, 2020; Zuzarte et al., 2024). Moreover, recent studies have highlighted the potential of these compounds as renewable

---

[*] Corresponding authors.
E-mail addresses: sergio.vilasboas@usc.es (S.M. Vilas-Boas), mcdcosta@unicamp.br (M.C. da Costa).
[1] These authors contributed equally to this work

https://doi.org/10.1016/j.psep.2026.108687

feedstocks for the production of fine chemicals (Sánchez-Velandia et al., 2025), biofuels (Lapuerta et al., 2023), bio-based polymers (Mukhtar Gunam Resul et al., 2023), and alternative solvents (Lindokuhle et al., 2026; Zhang et al., 2025). Taken together, these applications underscore the role of monoterpenes and their derivatives as emerging platform molecules within the modern biorefinery framework (Sánchez-Velandia et al., 2025). Despite their industrial versatility, however, many of these compounds are flammable.

To prevent accidents and mitigate fire and explosion (F&E) risks when handling flammable materials, adopting specific safety measures is essential (Sun et al., 2025). In this context, understanding key safety-related properties is paramount. One of the most widely recognized indicators for assessing F&E hazards is the flash point (FP), defined as the lowest temperature at which a liquid or liquid mixture releases sufficient vapor to form an ignitable mixture in the presence of a spark (Costa do Nascimento et al., 2024; Crowl and Louvar, 2011). This parameter is applied by regulatory institutions, such as the U.S. National Fire Protection Association (NFPA), to classify the flammability of liquids and to define standard safety protocols for the handling and storage of these substances and their mixtures (Costa do Nascimento et al., 2024; Vidal et al., 2006).

According to the Occupational Safety and Health Administration (OSHA), from the USA, any liquid or a liquid mixture with a FP at or below 93 °C is classified as flammable and subject to strict storage, handling, and transportation requirements (Occupational Safety & Health Administration [OSHA], 2012). Other agencies/legislations have their own thresholds, including differentiation between flammable (FP below 60°C) and combustible liquids (60°C < FP < 93°C), such as the US Department of Transportation, the European Union CLP Regulation, and the UN Globally Harmonized System. Although many industrially relevant substances fall into these categories, experimental FP data on complex organic mixtures remain scarce in the literature. Most available studies focus on the FP of fuel blends (Di Benedetto et al., 2018; Huo et al., 2022; Sosa et al., 2024) or organic solvent systems (De Liso et al., 2024; Lakzian and Liaw, 2021; Liaw et al., 2022; Liaw and Tang, 2025). Consequently, reliable data on other important high-added-value flammable mixtures are rarely reported in the open literature.

While the number of studies investigating the FP behavior of raw EOs is very limited (Cho et al., 2018; Guerrero et al., 2022; Rahman et al., 2019), systematic investigation into the FP of multicomponent mixtures representing their major terpenoid constituents remains remarkably scarce. To the best of our knowledge, there is only one previous study from our group (Vilas-Boas et al., 2023) that addressed the FP behavior of binary and ternary mixtures containing (R)-(+)-limonene, linalool, eucalyptol, and L-(–)-carvone, which are commonly found in EOs from citrus, caraway, and mint species. Many other commercial EOs are mainly composed of other monoterpenes, including mixtures of strongly associating phenolic monoterpenoids and aromatic hydrocarbons. The intricate structural features of these compounds introduce significant nonidealities and complex phase behavior that have not yet been systematically explored, currently limiting the reliability of F&E risk assessments for processes that handle such highly valuable materials.

To bridge this literature gap and build upon our previous work, this study investigates the FP behavior of four highly valuable and structurally complex monoterpenoids: *p*-cymene, linalool, carvacrol, and eugenol, alongside their binary and ternary mixtures over the entire composition range. These monoterpenoids are ubiquitous in commercially important EOs, supporting their use as representative model systems. For instance, linalool and eugenol are major constituents of cinnamon and basil EOs (Chericoni et al., 2005; Ilić et al., 2018; Muráriková et al., 2017; Raina et al., 2001; Schmidt et al., 2006; Stanojevic et al., 2019), while *p*-cymene and carvacrol are characteristic components of EOs from Mexican oregano (*Lippia origanoides*) (da Silva et al., 2024; Guimarães et al., 2021; Uc-Cachón et al., 2024) and various *Origanum* species (Baycheva and Dobreva, 2021; Kordali et al., 2008). Essential oils from winter savory (*Satureja montana* L.) are also notably rich in *p*-cymene, linalool, and carvacrol (Capdevila et al., 2025; Milos et al., 2001). Owing to their prevalence, mixtures of monoterpenes and monoterpenoids are often used as surrogate systems for studying EO thermophysical behavior (Vilas-Boas et al., 2023).

Although experimental thermophysical data are usually the preferred source, their acquisition is time-consuming and resource-intensive, especially for multicomponent mixtures requiring composition-dependent data (Costa do Nascimento et al., 2024). To overcome this challenge, various predictive approaches have been developed, including empirical, group contribution, quantitative structure-property relationship (QSPR), and thermodynamic-based models (Banihashemi and Movagharnejad, 2018; Jalaei Salmani et al., 2018; Le et al., 2015; Nazari et al., 2019; Phoon et al., 2014; Reinisch and Klamt, 2015; Torabian and Sobati, 2017). Among the thermodynamic approaches, the model proposed by Liaw et al. (Liaw et al., 2004, 2002), which integrates Le Chatelier's Rule with vapor-liquid equilibrium (VLE) principles, is widely applied to describe the FP of numerous systems (Costa do Nascimento et al., 2024; Phoon et al., 2014). This framework can be enhanced by coupling it with activity coefficient models to account for liquid-phase non-idealities, such as the UNIFAC (Fredenslund et al., 1975) or the quantum-chemistry-based COSMO-RS model (Eckert and Klamt, 2002; Klamt, 1995; Klamt et al., 1998). These combined approaches are particularly effective for complex, non-ideal systems.

In this work, we conducted experimental FP measurements for the four selected monoterpenes and their binary and ternary mixtures using the ASTM D6450 closed cup procedure, a method previously employed by our group for similar systems (Vilas-Boas et al., 2023). Whenever possible, the FP data obtained in this work were compared to data retrieved from the literature. Additionally, we performed FP predictions using the Liaw model (Liaw et al., 2004, 2002), considering both the ideal solution behavior and the UNIFAC model (Fredenslund et al., 1975) to represent liquid fugacity, and the COSMO-RS model (Reinisch and Klamt, 2015). This dual methodology enables a comprehensive evaluation of the FP of these important mixtures across experimental and theoretical approaches.

2. Materials and methods

2.1. Chemicals

Table 1 lists the compounds used in this work, including their CAS number, chemical structure, supplier, purity, and normal boiling point (NBP). All monoterpenoids were used as received from the suppliers, without further purification, and stored at room temperature in amber flasks.

2.2. Mixture preparation

All binary or ternary monoterpene mixtures were prepared gravimetrically to cover the entire composition range. Each mixture, with a total mass of approximately 5 g, was prepared in sealed amber flasks. The mass of each component was measured using an analytical balance (Shimadzu, AX200, reproducibility of $\pm 1 \times 10^{-4}$ g). After preparation, each mixture was homogenized by gentle stirring for 15 min and then allowed to reach thermal equilibrium at room temperature before use. To prevent moisture contamination, samples not immediately analyzed were stored in a desiccator until the measurements were performed.

2.3. Flash point measurements

The FP measurements were conducted using a Miniflash FLP/H/Touch analyzer (Grabner Instruments) following the ASTM D6450 continuously closed cup procedure (ASTM D6450–05 (2010)), an approach previously employed by our group (Costa do Nascimento et al., 2021; Vilas-Boas et al., 2023). The measured FP values were then

Table 1

CAS number, chemical structure, source, purity, and normal boiling point of the compounds used in this work. (Kobe et al#, 1941), (Lecat, 1928), (Kobe et al#, 1941), (Lecat, 1928), (Perry and Thodos, 1952).

Compound	CAS	Structure	Supplier	Purity (%)[a]	Normal boiling point (K)
p-cymene	2244-16-8	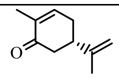	Sigma-Aldrich	≥ 99	449.65 (Kobe et al., 1941)
(±)-linalool	78-70-6	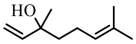	Sigma-Aldrich	≥ 97	471.80 (Lecat, 1928)
carvacrol	499-75-2	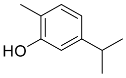	Acros Organics	≥ 98	510.45 (Kobe et al., 1941)
eugenol	97-53-0	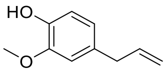	Alfa Aeser	≥ 99	528.15 (Lecat, 1928)
n-dodecane	14073-97-3	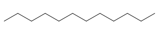	Sigma-Aldrich	≥ 99	489.40 (Perry and Thodos, 1952)

[a]The values correspond to the minimum purities granted by the manufacturer.

corrected to the standard atmospheric pressure (101.3 kPa) using Eq. (1):

$$FP_{corrected} = FP_{observed} + 0.25 * (101.3 - p) \quad (1)$$

where p is the ambient pressure (kPa) registered during each experiment. The atmospheric pressure data were provided for the Meteorological and Climatic Research Applied to Agriculture (CEPAGRI) at the Universidade Estadual de Campinas.

To ensure data reliability, each reported FP datapoint is the average of at least three independent measurements. Furthermore, the method accuracy was verified at the beginning of each workday by measuring the FP of a dodecane standard.

3. Modeling

3.1. The Liaw-UNIFAC combined approach

Among the frameworks for modeling the FP of homogeneous multicomponent mixtures, the method proposed by Liaw and co-authors (Liaw et al., 2004, 2002) is a benchmark approach due to its wide applicability (Costa do Nascimento et al., 2021; Phoon et al., 2014). The model is fundamentally based on combining the Le Chatelier empirical mixing rule with the vapor-liquid equilibrium (VLE) iso-fugacity criterion, where the VLE is described by the modified Raoult's law. For a mixture containing only flammable components, the Liaw method is expressed as (Liaw et al., 2004; Liaw and Yang, 2020):

$$\sum_{i=1}^{n}\frac{x_i\gamma_i p^{sat}_{i,FP_{mix}}}{p^{sat}_{i,FP}} = 1 \quad (2)$$

where x_i and γ_i are, respectively, the mole fraction and the activity coefficient of the component i in the liquid mixture, $p^{sat}_{i,FP_{mix}}$ is the vapor pressure of the pure component i at the mixture flash point temperature, and $p^{sat}_{i,FP}$ is the vapor pressure of the pure component i at its individual FP temperature.

The Liaw model accounts for liquid-phase nonidealities through the activity coefficients, γ_i, while assuming ideal behavior for the gas phase. This assumption is appropriate for the low-pressure conditions inherent to flash point measurements (Liaw et al., 2002). In this approach, the activity coefficients were estimated using the well-established UNIversal Functional Activity Coefficient (UNIFAC) model (Fredenslund et al., 1975). This group-contribution model was selected due to its predictive capabilities, as it does not require a regression of binary interaction parameters, unlike correlative approaches such as the NRTL and the Wilson models (Costa do Nascimento et al., 2020). A more detailed description of the Liaw-UNIFAC approach is available elsewhere (Liaw et al., 2011). For comparison, flash point predictions assuming ideal solution behavior (i.e., $\gamma_i = 1$ for all components) were also performed with the Liaw model.

Moreover, the vapor pressure data required for the Liaw model, p_i^{sat} and $p^{sat}_{i,FP}$, were calculated using the Antoine equation, expressed as follows:

$$\ln(p^{sat}) = \quad A - \frac{B}{T + C} \quad (3)$$

where p^{sat} is the vapor pressure (in Pa), T is the absolute temperature (in K), and A, B, and C are the Antoine's parameters for the component i. The vapor pressure of the pure component i at its own FP temperature ($p^{sat}_{i,FP}$) and at the mixture FP temperature ($p^{sat}_{i,FP_{mix}}$) are obtained by applying the corresponding temperatures ($T_{i,FP}$ and T_{FPmix}) in Eq. (3). This empirical approach is widely used due to its simplicity and accuracy when its coefficients are regressed from data within the temperature range of interest (Costa do Nascimento et al., 2024). The Antoine parameters for each monoterpenoid were determined by regressing experimental vapor pressure data collected from an extensive literature survey (Clará et al., 2009; Deng et al., 2002; Lecat, 1927; Linder, 1931; Mcdonald et al., 1959; Qin et al., 2022; Rodrigues et al., 2022; Russo et al., 2019; Štejfa et al., 2023; Stull, 1947; Vilas-Boas et al., 2019; Zaitsau et al., 2015). The resulting regressed Antoine coefficients are provided in Table S1 of the Supplementary Material (SM). All the Liaw-UNIFAC calculations were performed using the Flash Point Multicomponent – Methods and Algorithm (FLAMMA) software, described in detail in our previous work (Costa do Nascimento et al., 2021). This algorithm has been successfully applied to describe the FP of several binary and multicomponent mixtures (Sosa et al., 2024; Vilas-Boas et al., 2023).

3.2. COSMO-RS

The Conductor-like Screening Model for Real Solvents (COSMO-RS) is a predictive thermodynamic model that combines quantum chemistry with statistical thermodynamics to calculate the chemical potential of molecules in liquid systems (Eckert and Klamt, 2002; Klamt, 1995; Klamt et al., 1998). The method relies on two sequential steps. First, a quantum-chemical calculation is performed for each individual molecule using the COSMO solvation model, which embeds the molecules within a virtual perfect conductor. This initial step yields the molecule's screening polarization charge density (σ) on its surface and its corresponding geometry and energy. The charge density information is then converted into a histogram, known as the σ-profile, which serves as a detailed descriptor of the molecule's polarity. In the second step, statistical thermodynamics is applied to compute the chemical potentials, based on pairwise interactions between the surface segments of the molecules in the ensemble (Klamt et al., 2019, 2010). From the chemical potentials, the activity coefficients of each compound in the mixture are derived (Klamt and Eckert, 2000), enabling the prediction of other important physicochemical properties (e.g., partition coefficients, separation factors, solubilities). Furthermore, the model is also capable of predicting pure component thermophysical properties, such as vapor pressures and enthalpies of vaporization, from the chemical potential difference between the liquid and ideal gas phases (Lin et al., 2004). More details on COSMO-RS fundamentals are available in previous works from Klamt and co-authors (Klamt, 2011, 2005; Klamt et al., 2010).

A key advantage of COSMO-RS is its ability to predict a wide range of physicochemical and equilibrium properties without extensive sets of experimental data or system-specific fitted parameters. For terpene-containing mixtures, the model has been successfully applied to describe properties such as activity coefficients at infinite dilution (Vilas-Boas et al., 2023a; Zambom et al., 2023), solubilities (Vilas-Boas et al., 2023b, 2022), solid-liquid phase diagrams (Teixeira et al., 2022), partition coefficients (Lorenzo-Llanes et al., 2025; Vilas-Boas et al., 2025), liquid-liquid equilibrium (Ozturk and Gonzalez-Miquel, 2019), boiling points (Dupeux et al., 2022), and flash point (Vilas-Boas et al., 2023).

To compute the FP for mixtures of flammable compounds, COSMO-RS employs a modified version of Liaw's approach, expressed as (Reinisch and Klamt, 2015):

$$\frac{1}{\left(T^{f}-T_{FPmix}\right)}\sum_{i}\frac{x_{i}\gamma_{i}p^{sat}_{i,FP_{mix}}\left(T^{f}-T_{i,FP}\right)}{p^{sat}_{i,FP_{i}}}=1 \tag{4}$$

where T^f is the flame temperature (a parameter set by default at 1573 K), T_{FPmix} is the mixture FP temperature, $T_{i,FP}$ is the FP temperature of the pure compound i, p^{sat}_{i,FP_i} is the vapor pressure of the pure compound i at $T_{i,FP}$, $p^{sat}_{i,FP_{mix}}$ is the vapor pressure of the pure compound i at T_{FPmix}, and x_i and γ_i are the mole fraction and the activity coefficient of the component i, respectively.

In this framework, the γ_i values are calculated as a function of composition (x_i) and temperature (T) directly from the chemical potentials predicted for each individual compound in the mixture. Regarding the pure component parameters (and $T_{i,FP}$), the model offers flexibility: they can either be experimental values or purely predictive estimates. When considering predicted $T_{i,FP}$ values, they are obtained from a direct correlation between the compound's vapor pressure and its molecular surface area derived from the COSMO optimization (Reinisch and Klamt, 2015).

The COSMO-RS calculations were performed using its implementation in the COSMOtherm software package (version 21.0) (BIOVIA COSMOtherm, 2021; Eckert and Klamt, 2002) with the BP_TZVPD_FINE_21.ctd parametrization. Since the files with the required input information (i.e., screening polarization charge density, geometry coordinates, and energies) were not available in the default COSMOtherm database, they were generated using the COSMOConf (version 2021) (BIOVIA COSMOconf 21, 2021) coupled with TmoleX software (Steffen et al., 2010), following the COSMO-BP-TZVPD-FINE template. The full set of generated conformers by COSMOconf was considered in all COSMOtherm calculations.

The experimental FP values of the pure monoterpenes measured in this work were used as input in the COSMO-RS calculations for the mixtures, as there is evidence that this procedure leads to substantially improved description of the FP behavior of terpene mixtures (Vilas-Boas et al., 2023). The vapor pressures and activity coefficients predicted by the model were used to compute the FP of mixtures via Eq. (4). Further details on the calculation procedure are available in the COSMOtherm reference manual (BIOVIA COSMOtherm, 2020, 2020).

3.3. Statistical analysis

To quantitatively assess the performance of the thermodynamic models, deviations between the experimental ($T^{exp}_{FP,j}$) and predicted ($T^{calc}_{FP,j}$) flash point values were calculated. In this work, the primary metric was the root-mean-square error (RMSE), calculated as:

$$\mathrm{RMSE}=\sqrt{\left[\frac{\sum_{j}\left(T^{exp}_{FP,j}-T^{calc}_{FP,j}\right)^{2}}{n}\right]} \tag{5}$$

where superscripts ″exp″ and "*calc*″ correspond to the experimental and calculated values, respectively, n is the total number of data points, and j denotes each specific datapoint.

4. Results and discussion

4.1. Pure compounds

In Table 2, the experimental FP values measured for the four monoterpenoids (*p*-cymene, linalool, carvacrol, and eugenol) and the reference compound (*n*-dodecane) are compared with data collected from the literature. Each value reported from herein represents the average of at least three independent measurements, with the standard deviations indicated by the ± signs. Due to the scarcity of data for the monoterpenoids in peer-reviewed scientific papers, values from suppliers' technical reports were also included to provide a broader comparison.

The high precision of the experimental measurements is confirmed by the low coefficients of variation, which were below 0.2% for all the compounds. Furthermore, the FP value obtained for *n*-dodecane showed excellent agreement with literature data, confirming the reliability of the experimental procedure. Regarding the pure monoterpenoids, the available FP data exhibit some variability. For eugenol, literature values range from 377.2 to 400.2 K, and the value obtained in this work (394.7

Table 2
Overview of the experimental FPs measured in this work (at 101.3 ± 0.5 kPa) and values found in the literature.

Compound	FP – this work (K)	FP – literature (K)
p-cymene	328.4 ± 0.1	325.2 (Sigma-Aldrich, 2024)
linalool	354.6 ± 0.5	353.1 ± 0.1 (Vilas-Boas et al., 2023); 350.4 (Sigma-Aldrich, 2022); 349.15 (Clark, 1988); 344.3 (Api et al., 2015)
carvacrol	385.1 ± 0.5	379.2 (ThermoFisher Scientific, 2022)
eugenol	394.7 ± 0.8	400.2 (University of Hertfordshire, 2025); 397.2 (Sigma-Aldrich, 2023); 377.2 (Yuwono et al., 2002)
dodecane	354.2 ± 0.3	354.5 ± 0.6 (Vilas-Boas et al., 2023); 354.4 ± 0.1 (Henriques et al., 2020); 354.4 ± 0.4 (Costa do Nascimento et al., 2021); 354.2 (Li et al., 2014); 352.5 ± 2 K (Luning Prak et al., 2017)

± 0.8 K) falls within this range. In the case of linalool, our measured FP (354.6 ± 0.5 K) is in close agreement with our previous work (353.1 ± 0.1 K), and slightly higher than the values found in other sources (Api et al., 2015; Clark, 1988; Sigma-Aldrich, 2022). For *p*-cymene and carvacrol, no data were found in peer-reviewed manuscripts; however, values reported in technical reports from suppliers are slightly lower than those measured in this study.

Variations among reported FP values in the literature are common and often attributable to the experimental methodology employed (Rowley et al., 2010). The most common methodologies to determine experimental FP data are generally categorized into open-cup and closed-cup tests. While open-cup methods are suitable for less volatile substances, closed-cup methods are recommended for volatile compounds as they prevent the loss of flammable vapors, thus providing more consistent and reliable data (Hshieh and Hshieh, 2005; Phoon et al., 2014). Consequently, FP values for the same substance measured by different techniques can differ by several degrees (Haghtalab et al., 2016; Phoon et al., 2014). This context is crucial for evaluating the data presented in Table 2, as most of the cited sources do not specify the method used.

Notably, the values from the sources that explicitly employed the closed-cup methods, namely our previous work (Vilas-Boas et al., 2023) and the technical reports from Sigma-Aldrich, are in excellent agreement with the data reported here, exhibiting relative deviations below 1.2%. Furthermore, the overall variability observed for the monoterpenoids in this study is comparable to that reported in previous work for other flammable substances, which further supports the reliability of our results (Lakzian and Liaw, 2021, 2024; Liaw et al., 2022; Sosa et al., 2024; Vilas-Boas et al., 2023).

Nonetheless, notable differences are observed when comparing our data with certain literature values, particularly for carvacrol and eugenol. Regarding carvacrol, the experimental FP measured in this work (385.1 ± 0.5) K is approximately 6 K higher than the value listed in the ThermoFisher Scientific (2022) technical report. For eugenol, while our result (394.7 ± 0.8) K aligns well with the value reported by Sigma-Aldrich (397.2) K, which was measured through a closed-cup method, substantial deviations are found regarding the values reported by Yuwono et al., (2002) (377.2 K) and the University of Hertfordshire database (400.2) K. Crucially, neither the ThermoFisher report for carvacrol nor the sources presenting the most divergent values for eugenol (University of Hertfordshire, 2025; Yuwono et al., 2002) specify the experimental apparatus or methodology employed. Moreover, it is well established that FP is a method-dependent property (Rowley et al., 2010); consequently, values obtained using different operational procedures or apparatuses cannot be readily correlated. Therefore, the observed differences in the FP values of these monoterpenoids are likely attributable to differences in testing protocols or variations in sample purity.

The FP values obtained in this work for the monoterpenoids follow the same trends as their normal boiling point (NBP) values: *p*-cymene < linalool < carvacrol < eugenol. This observation is consistent with our previous work, which reported a similar behavior for the other three monoterpenoids: (R)-(+)-limonene, eucalyptol, and L-(–)-carvone (Vilas-Boas et al., 2023). Indeed, strong empirical correlations between FP and NBP have been proposed for various organic families, including hydrocarbons, alcohols, acids, esters, ketones, and aldehydes (Carroll et al., 2011; Patil, 1988). To illustrate this behavior for the monoterpenoids investigated, Fig. 1 compares the experimental FP values from this study and our previous work with their respective NBP values. A strong linear relationship ($R^2 = 0.983$) was observed, and the regression of the data resulted in the following correlation: $FP = 0.876 \times NBP - 65.680$. This correlation holds across a diverse set of chemical families, including an alcohol (linalool), phenols (eugenol and carvacrol), a ketone (carvone), an ether (eucalyptol), and hydrocarbons (*p*-cymene and limonene). Although the number of datapoints is limited ($n = 7$), the simple correlation offers a valuable tool for providing a rapid, first-estimate of the FP for other monoterpenes with known boiling points in the 420–530 K range.

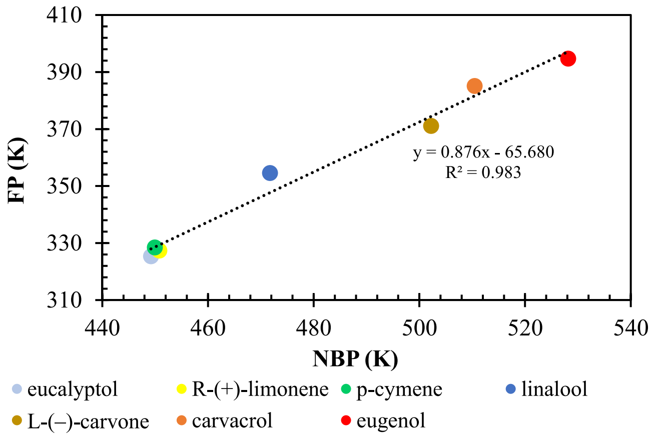

Fig. 1. Correlation between the experimental flash point and the normal boiling point for the studied monoterpenoids. Data sourced from Table 1 and (Vilas-Boas et al., 2023).

As noted in Section **3.2**, COSMO-RS can also be applied to predict the FP behavior of pure compounds (Reinisch and Klamt, 2015). For comparison, the FP data predicted with the proposed linear FP-NBP correlation are benchmarked against the values predicted with COSMO-RS in Figure S1 of the SM. Two scenarios were considered for the COSMO-RS predictions: Approach 1 (fully predicted FP data from the molecular surface) and Approach 2 (FP predicted using experimental NBP as input data).

The linear FP-NBP correlation yielded the lowest global deviations (RMSE = 3.5 K), followed by COSMO-RS Approach 2 (RMSE = 4.1 K) and Approach 1 (RMSE = 5.0 K). Notably, these deviations are comparable to discrepancies often found between experimental data from different sources (Table 2**)**, particularly when different experimental methodologies are employed. Furthermore, since deviations up to 5–8 K are not unusual for experimental FP data obtained using well-established methods (Phoon et al., 2014), these results suggest that these approaches are valid for estimating the FP of monoterpenes, especially given the scarcity of reliable experimental data.

4.2. Binary mixtures

The experimental FP data measured for the six binary mixtures studied in this work (i.e., *p*-cymene + linalool, *p*-cymene + carvacrol, *p*-cymene + eugenol, linalool + carvacrol, linalool + eugenol, and carvacrol + eugenol) are presented in Table 3. For each system, six mixtures were analyzed, covering a mole fraction range from ($0.1 \leq x_i \leq 0.9$). The high precision of the measurements was confirmed by the low standard deviations (≤ 1.3 K) and a maximum coefficient variation of 0.34%.

Fig. 2 presents a comparison of the experimental FP values with the predictions from the three studied modeling approaches investigated in this work: the ideal approach, the Liaw-UNIFAC model, and the COSMO-RS model. In all plots, the *x*-axis represents the mole fraction of the component with the lower FP value in the mixture. A quantitative overview of each model's performance is presented in Fig. 3, which summarizes the RMSE for each binary system. The list of RMSE values obtained for all predictive approaches is presented in Table S2 of the SM.

For all binary systems, the experimental FP value decreases as the mole fraction of the volatile component increases, a trend commonly reported for binary mixtures of terpenes (Vilas-Boas et al., 2023) and other compounds (Dias et al., 2019; Li et al., 2014; Sosa et al., 2024). However, the deviations from the ideal model prediction reveal crucial

Table 3
Experimental flash points of the binary terpene mixtures studied in this work.[a].

linalool (1) + *p*-cymene (2)		**carvacrol (1) + *p*-cymene (2)**	
x_1	**FP (K)**[b]	x_1	**FP (K)**[b]
0	328.4 ± 0.1	0	328.4 ± 0.1
0.101	329.7 ± 0.4	0.101	330.3 ± 0.5
0.201	330.8 ± 0.5	0.202	332.0 ± 0.5
0.400	333.5 ± 0.1	0.402	335.0 ± 0.7
0.599	337.2 ± 0.5	0.602	340.2 ± 0.5
0.801	342.6 ± 0.1	0.800	350.5 ± 0.1
0.901	347.2 ± 0.5	0.901	361.7 ± 0.5
1	354.4 ± 0.1	1	385.1 ± 0.5
eugenol (1) + *p*-cymene (2)		**carvacrol (1) + linalool (2)**	
x_1	**FP (K)**[b]	x_1	**FP (K)**[b]
0	328.4 ± 0.1	0	354.4 ± 0.1
0.101	329.8 ± 0.5	0.104	356.1 ± 0.9
0.208	332.2 ± 0.5	0.200	358.5 ± 0.1
0.403	335.6 ± 0.7	0.400	364.2 ± 0.5
0.600	340.3 ± 0.5	0.599	371.0 ± 0.5
0.795	349.4 ± 0.5	0.797	378.7 ± 0.1
0.901	366.3 ± 1.3	0.901	381.9 ± 0.8
1	394.7 ± 0.8	1	385.1 ± 0.5
eugenol (1) + linalool (2)		**eugenol (1) + carvacrol (2)**	
x_1	**FP (K)**[b]	x_1	**FP (K)**[b]
0	354.4 ± 0.1	0	385.1 ± 0.5
0.103	356.0 ± 0.9	0.101	385.8 ± 0.5
0.201	357.4 ± 0.5	0.202	386.5 ± 0.1
0.400	361.7 ± 0.1	0.402	388.2 ± 0.5
0.603	367.0 ± 0.5	0.706	390.7 ± 0.1
0.800	375.7 ± 0.7	0.798	391.8 ± 0.8
0.897	382.7 ± 0.7	0.901	393.1 ± 0.5
1	394.7 ± 0.8	1	394.7 ± 0.8

[a] Relative standard uncertainty on the mole fractions is: $u^r(x) = 0.003$. [b] Standard deviations are placed after the plus-minus sign.

information about the governing intermolecular interactions.

The three systems with *p*-cymene exhibit experimental FP values lying significantly below the ideal prediction (2.7 K ≤ RMSE ≤ 5.3 K). Such observations indicate a positive deviation from Raoult's law ($\gamma_i > 1$), suggesting that repulsive forces predominate and the interactions between *p*-cymene and the other components are weaker than the self-interactions of the pure compounds. The observed behavior is consistent with our previous work on hydrocarbon/oxygenated monoterpene mixtures (Vilas-Boas et al., 2023).

A different behavior is observed for the mixtures composed solely of oxygenated monoterpenes. The linalool + carvacrol mixture shows experimental FP values substantially above the ideal curve (RMSE = 4.4 K), indicating a negative deviation from Raoult's law ($\gamma_i < 1$). In this system, attractive forces are dominant, likely due to hydrogen bonding between the hydroxyl (–OH) groups of linalool and carvacrol. Conversely, the linalool + eugenol and carvacrol + eugenol systems exhibit experimental FP lying slightly below the ideal prediction, achieving RMSE values of 1.5 and 1.1 K, respectively. The latter reflects a near-ideal behavior, suggesting that repulsive forces are only marginally dominant. This likely occurs because the eugenol's ability to form intermolecular hydrogen bonds is reduced by a competing intramolecular bond formed between its hydroxyl (–OH) and methoxy (–OCH_3) groups (Shen et al., 2023).

When comparing the performance of the predictive models, COSMO-RS provides the best overall description for all binary mixtures. This is evidenced by its low global RMSE of 0.8 K and individual RMSE values that did not exceed 1.5 K for any system. The model's strength is particularly evident in describing the FP of the mixtures with strong deviation from ideality (i.e., *p*-cymene + eugenol, linalool + carvacrol, *p*-cymene + carvacrol), where it achieved RMSE values that were more than 70% lower than those from the ideal approach. These results align well with our previous work, which also reported superior performance of COSMO-RS for binary mixtures containing terpenes, including (R)-(+)-limonene, eucalyptol, linalool, and L-(–)-carvone (Vilas-Boas et al., 2023).

On average, the Liaw-UNFICAC model offers a slight improvement over the simple ideal approach, with global RMSE values are 2.7 K and 3.0 K, respectively. Its performance varies across the different studied systems. For mixtures containing *p*-cymene, the Liaw-UNIFAC model successfully captures the direction of the non-ideality, providing accurate descriptions for the *p*-cymene + linalool (RMSE = 0.8 K) and *p*-cymene + carvacrol (RMSE = 1.6 K). The model is less accurate, however, for the *p*-cymene + eugenol mixture, where it overestimates the repulsive interactions, resulting in a comparatively high RMSE of 6.4 K. For the oxygenated mixtures, the Liaw-UNIFAC provides a better representation than the ideal approach for the linalool + carvacrol mixture (RMSE = 3.5 K vs 4.4 K). Conversely, for the two mixtures containing eugenol (linalool + eugenol and carvacrol + eugenol), the model was slightly less accurate than the ideal approach.

The comparison of models' performances in describing the FP behavior of binary mixtures aligns well with theoretical fundamentals. The ideal approach assumes that interactions between unlike molecules are energetically equivalent to those of the individual compounds (Prausnitz et al., 1999). Consequently, this model provides accurate descriptions only for mixtures with similar polarity. Experimental FP data confirm this expectation: while eugenol + oxygenated monoterpene mixtures are well described, significant deviations are observed for the linalool + carvacrol and the *p*-cymene-containing systems. These deviations stem from factors ignored by the ideal framework: the repulsive interactions between nonpolar hydrocarbon and polar hydroxyl groups in systems with *p*-cymene, and the strong attractive interactions (hydrogen bonding) in the linalool + carvacrol mixture. In contrast, in the eugenol + carvacrol/linalool systems, eugenol's tendency to form intramolecular hydrogen bonds (Shen et al., 2023) likely attenuates the overall intermolecular interactions, resulting in behavior closer to ideality.

Unlike the ideal approach, UNIFAC accounts for solution non-idealities via activity coefficients obtained from group-contribution parameters (Poling et al., 2001). However, the model assumes that functional group contributions are additive and independent (Fredenslund et al., 1975), which limits its accuracy for systems with strong specific interactions (e.g., hydrogen bonds) or proximity effects (Kontogeorgis and Folas, 2010; Poling et al., 2001). While the Liaw-UNIFAC performs well where cross-association is absent (*p*-cymene + linalool/carvacrol), it overpredicts associative interactions when hydrogen bonding dominates. Notably, the model's inability to account for intramolecular shielding is evident for the p-cymene + eugenol mixture. By treating the hydroxyl as fully available, the model strongly overpredicts repulsion, yielding FP predictions lower than the experimental values. Furthermore, standard UNIFAC parameters are regressed from a large database of equilibrium data that may lack sufficient representation of structurally similar species to the monoterpenes studied here. While this broad generalization is a major advantage for systems lacking experimental data, it inherently limits the model precision when describing nuanced, highly specific interactions of intricate molecules.

In contrast, COSMO-RS predicts mixture non-idealities based on the screening charge density (σ) of the molecular surfaces determined by quantum chemistry (Klamt et al., 2010). This allows it to capture structural features that empirical methods miss, including the role of multiple conformers in flexible molecules like eugenol (Olbert-Majkut and Wierzejewska, 2008). The capability explains its superior performance for the *p*-cymene + eugenol system: by incorporating conformers stabilized by intramolecular hydrogen bonds, COSMO-RS correctly predicts a reduced surface polarity and a more accurate representation of repulsive interactions. Similarly, for the linalool + carvacrol model, where cross-association is dominant, the model offers a significantly improved representation of the FP behavior compared to Liaw-UNIFAC and the ideal approach.

It is noteworthy that flammable mixtures with FP profiles below the ideal behavior require special attention from safety and handling

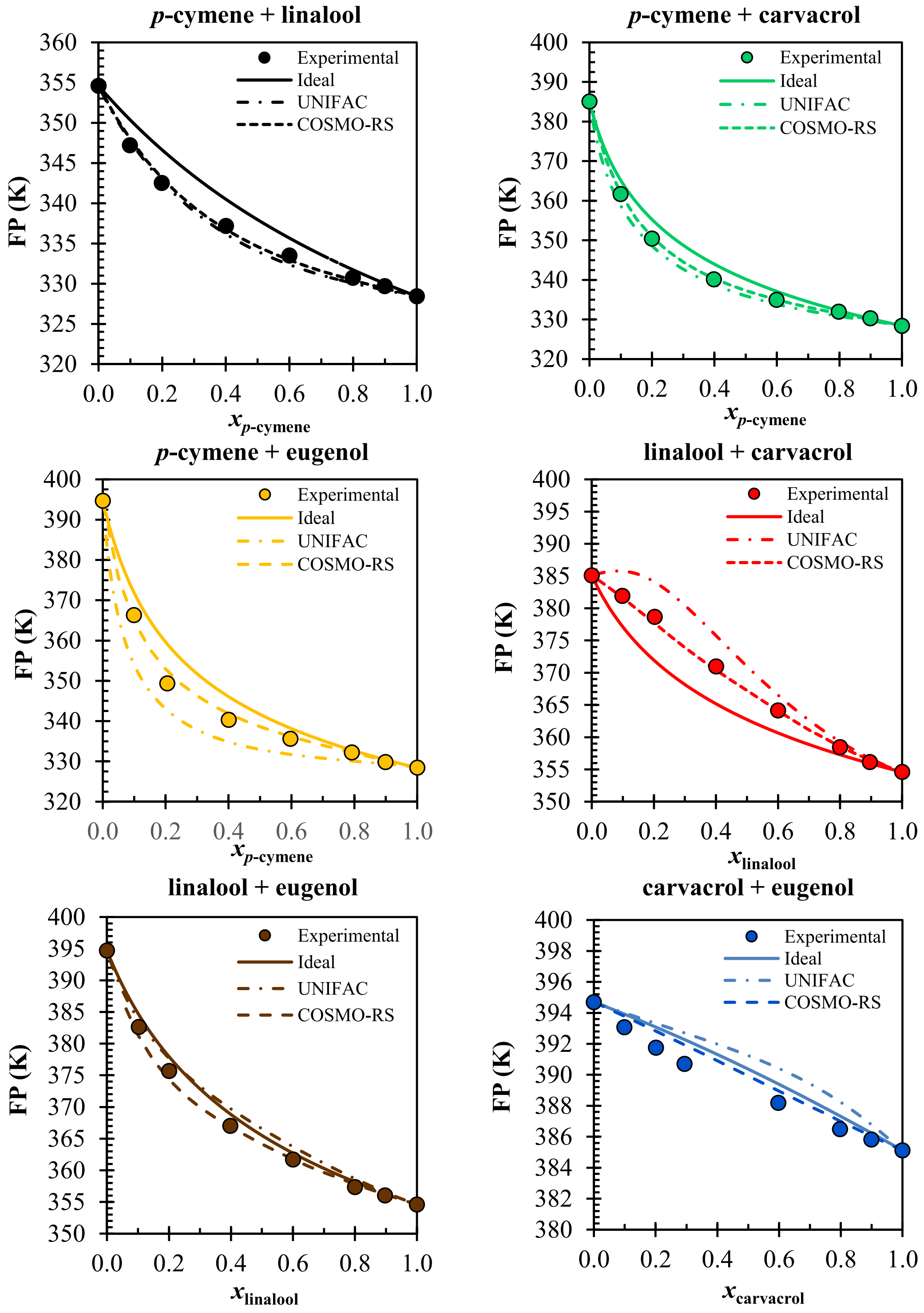

Fig. 2. Comparison of the experimental FP values with the predicted profiles for the studied mixtures.

perspectives, as a failure to account for such non-idealities could lead to an underestimation of the actual fire hazard. This study provides key examples of this situation. One is the *p*-cymene + carvacrol binary mixture, common in essential oils from *Lippia origanoides* and *Origanum* species (Baycheva and Dobreva, 2021; Guimarães et al., 2021; Kordali et al., 2008; Uc-Cachón et al., 2024), which exhibits FP values significantly lower than those ideally predicted; relying on the ideal model would lead to an overestimation of the FP by up to 5 K. Similarly, the linalool + eugenol mixture, abundant in EOs from cinnamon and basil species (Chericoni et al., 2005; Ilić et al., 2018; Muráriková et al., 2017; Raina et al., 2001; Schmidt et al., 2006; Stanojevic et al., 2019), also exhibits experimental FPs lower than the ideal values. In both cases, underestimating flammability can lead to unsafe handling conditions, underscoring the importance of applying a robust thermodynamic model, such as COSMO-RS, for accurate industrial safety assessments.

4.3. *Ternary mixtures*

The experimental FP data measured for the four ternary monoterpene mixtures (i.e., *p*-cymene + linalool + carvacrol, *p*-cymene +

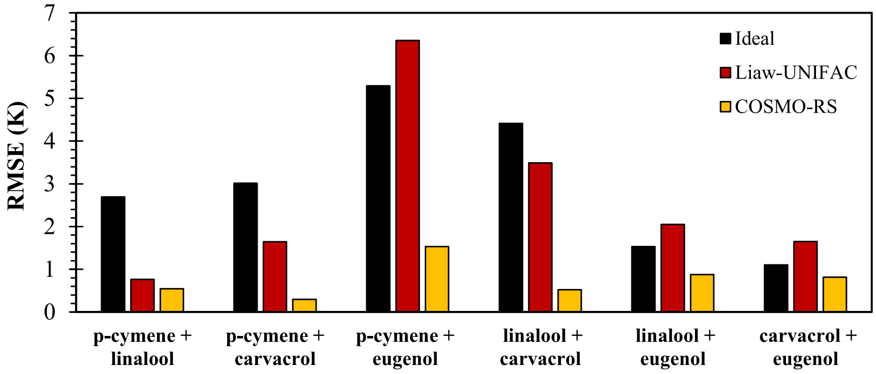

Fig. 3. Overview of the root-square mean errors (RMSE) obtained between the experimental and predicted FP values of the binary terpene mixtures.

linalool + eugenol, *p*-cymene + carvacrol + eugenol, linalool + carvacrol + eugenol) are listed in Table 4. To efficiently map the compositional space of these systems, a simplex-lattice design method strategy (Cornell, 2002) was adopted. A lattice degree of $m = 5$ was selected, establishing a primary grip spacing of $\Delta x = 0.2$. In addition to the primary nodes, a few extra measurements were conducted for intermediate compositions (i.e., $\Delta x_i \approx 0.1$). This methodological approach has already been employed in previous works from our group (Costa do Nascimento et al., 2021; Sosa et al., 2024; Vilas-Boas et al., 2023). The high precision of the measurements was confirmed by the low standard deviations (always below 1.2 K) and a maximum coefficient variation of 0.33%.

The three modeling approaches previously used for the binary systems (COSMO-RS, Liaw-UNIFAC, and the ideal approach) were also applied to the ternary mixtures. The results are presented in Figs. 4–6, where the experimental FP data are compared with the values predicted by the models. A quantitative overview of each model's performance is presented in Fig. 7, which summarizes the RMSE values for each ternary system (detailed results are listed in Table S3).

Table 4
Experimental flash point data of the ternary mixtures studied in this work.[a].

***p*-cymene (1) + linalool (2) + carvacrol (3)**			***p*-cymene (1) + linalool (2) + eugenol (3)**		
x_1	x_2	**FP (K)**[b]	x_1	x_2	**FP (K)**[b]
1	0	328.4 ± 0.1	1	0	328.4 ± 0.1
0	1	354.4 ± 0.1	0	1	354.4 ± 0.1
0.201	0.200	348.7 ± 0.1	0.210	0.209	347.0 ± 0.5
0.200	0.405	346.0 ± 0.5	0.205	0.410	345.7 ± 0.7
0.201	0.602	343.8 ± 0.8	0.201	0.603	344.0 ± 0.5
0.401	0.200	338.9 ± 0.5	0.408	0.205	338.4 ± 0.2
0.399	0.402	337.2 ± 0.5	0.402	0.402	337.4 ± 0.5
0.603	0.199	333.4 ± 0.5	0.604	0.201	333.7 ± 0.5
0.798	0.102	330.8 ± 0.7	0.803	0.100	331.0 ± 0.9
0.097	0.805	348.9 ± 0.4	0.099	0.803	348.6 ± 0.9
0.101	0.098	360.3 ± 0.5	0.105	0.105	358.0 ± 0.5
0	0	385.1 ± 0.5	0	0	394.7 ± 0.8
***p*-cymene (1) + carvacrol (2) + eugenol (3)**			**linalool (1) + carvacrol (2) + eugenol (3)**		
x_1	x_2	**FP (K)**[b]	x_1	x_2	**FP (K)**[b]
1	0	328.4 ± 0.1	1	0	354.4 ± 0.1
0	1	385.1 ± 0.5	0	1	385.1 ± 0.5
0.196	0.212	349.7 ± 0.1	0.202	0.193	376.7 ± 0.5
0.196	0.413	349.9 ± 0.5	0.204	0.384	376.1 ± 0.7
0.199	0.600	351.1 ± 0.4	0.212	0.576	377.1 ± 0.1
0.397	0.205	340.2 ± 0.5	0.403	0.194	366.7 ± 0.5
0.396	0.405	340.2 ± 0.5	0.412	0.383	368.6 ± 1.1
0.596	0.205	335.4 ± 1.1	0.600	0.197	362.1 ± 0.1
0.799	0.103	331.9 ± 0.7	0.797	0.102	356.7 ± 0.5
0.099	0.800	361.9 ± 0.1	0.111	0.780	380.8 ± 0.5
0.101	0.107	361.6 ± 0.5	0.101	0.094	381.9 ± 0.8
0	0	394.7 ± 0.8	0	0	394.7 ± 0.8

[a]Relative standard uncertainty on the mole fractions is: $u^r(x) = 0.003$. [b]Standard deviations are placed after the plus-minus sign.

The experimental and modeling results for the ternary mixtures confirm the trends observed for the binary systems. The mixture FP decreases as the mole fraction of the more volatile component increases, a trend captured by all three modeling approaches. COSMO-RS again provided the best representation of the FP profiles, achieving a low global RMSE of 1.0 K. Its individual RMSE values ranged from a highly accurate 0.6 K (*p*-cymene + linalool + carvacrol) to a maximum of 1.7 K (*p*-cymene + carvacrol + eugenol). The Liaw-UNIFAC model (global RMSE = 3.2 K) was, once more, superior to the ideal approach (global RMSE = 4.2 K). The model performed particularly well for the mixtures containing *p*-cymene and linalool, achieving RMSE values of 0.9 K for *p*-cymene + linalool + carvacrol and 2.2 K for *p*-cymene + linalool + eugenol.

The performance of the models varied significantly with the chemical nature of the mixture. For the three systems containing the hydrocarbon *p*-cymene, the ideal model performed more poorly (RMSE ranging from 3.4 to 6.1 K) than the other two models. As with the binary mixtures, it consistently predicted FPs that were higher than the experimental values; however, both COSMO-RS and Liaw-UNIFAC correctly predicted FPs lower than the ideal values, providing better FP descriptions of these systems (Fig. 7).

A distinct behavior was observed in the ternary system containing only oxygenated terpenes (linalool, carvacrol, and eugenol). In this case, the ideal model (RMSE = 2.2 K) outperformed the Liaw-UNIFAC model (RMSE = 4.4 K).

As previously discussed for the binary mixtures, the trends observed in the predictive performance of the assessed models agree with their thermodynamic fundamentals. Once more, the ideal approach exhibits a poor performance in describing the FP behavior of the ternary systems containing *p*-cymene, a direct consequence of its inability to predict the repulsive interactions between this nonpolar hydrocarbon and the oxygenated monoterpenes. Conversely, its better performance in describing the linalool + carvacrol + eugenol FP behavior is likely a consequence of eugenol's intramolecular hydrogen-bonding effect (Shen et al., 2023). This shielding effect partially reduces the overall attractive forces within the complex multicomponent matrix, bringing the system closer to ideality than the binary carvacrol + linalool system.

While the Liaw-UNIFAC model correctly captures the direction of the deviations from ideality across all ternary systems, its quantitative accuracy is highly system-dependent. For mixtures with *p*-cymene, the model offers a very good representation of the *p*-cymene + linalool + carvacrol system, where intramolecular interactions are absent. Its performance drops considerably when eugenol is introduced to the system. While the model generally underpredicts the FP of ternary mixtures containing *p*-cymene and eugenol, as a result of an overestimation of the repulsive forces, the opposite effect is observed for the mixture composed solely of the three oxygenated compounds. For this

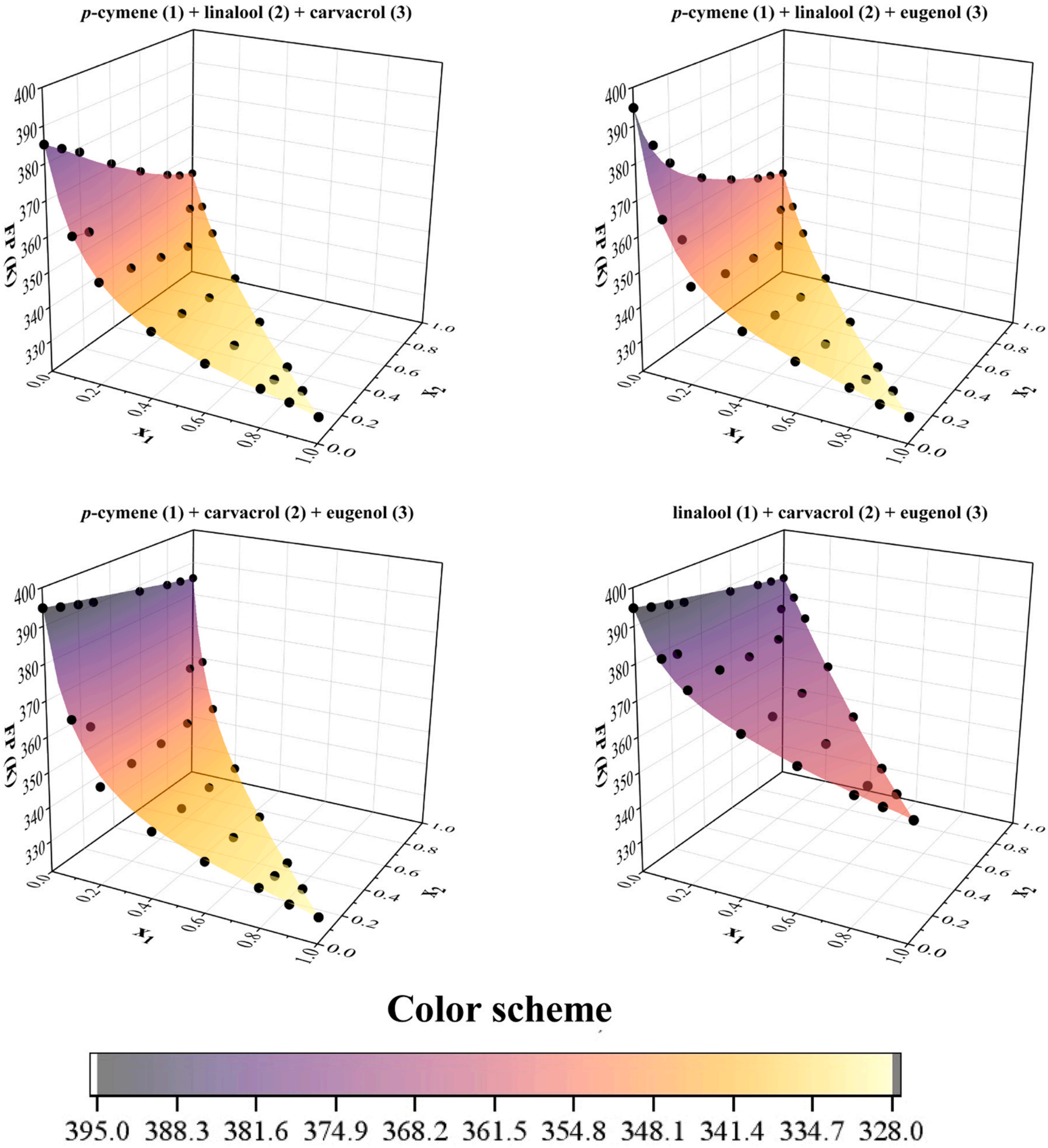

Fig. 4. Comparison of experimental FP values (●) with the profiles predicted by the COSMO-RS model for the studied ternary mixtures.

mixture, the Liaw-UNIFAC overestimates the strength of the attractive cross-interactions, predicting FPs even higher than the ideal values. This behavior likely results from the lack of specific parameters to account for intramolecular hydrogen-bond interactions (Campbell and Luthy, 1985; De Las Heras López et al., 2023), causing the model to treat all hydroxyl groups as fully available for intermolecular bonding.

On the other hand, the excellent performance of COSMO-RS, which outperforms both Liaw-UNIFAC and the ideal approach in all four ternary systems, is attributed to its ability to better account for complex interactions, including intramolecular and intermolecular hydrogen bonding. The model's capacity to incorporate multiple conformations in the calculation of thermophysical properties is a key factor in capturing the nonidealities of complex multicomponent systems. The results found in this work confirm the reliability of COSMO-RS as a predictive tool for the FP of terpene mixtures, aligning well with our previous results for both FP and other thermophysical properties of mixtures containing monoterpenes (Vilas-Boas et al., 2025; Vilas-Boas et al., 2023; Vilas-Boas et al., 2023b, 2022). Nonetheless, the group-contribution Liaw-UNIFAC model also has its merits; although it performs worse than COSMO-RS, it successfully captures nonideal trends and provides improved global predictions compared to the ideal approach for most of the studied mixtures. Furthermore, it is a conceptually simpler model than COSMO-RS, with its required parameters being freely available (Dortmund Data Bank [WWW Document], 2025).

The practical importance of using a robust thermodynamic model is best illustrated by the ternary system composed of *p*-cymene, linalool, and carvacrol, a mixture representative of EOs from winter savory (Capdevila et al., 2025; Milos et al., 2001). For this system, the ideal approach predicts FPs significantly higher than the experimental data (RMSE = 3.4 K). In contrast, substantially improved predictions were obtained with COSMO-RS (RMSE = 0.6 K) and the Liaw-UNIFAC model (RMSE = 0.9 K), highlighting their value in accurate process safety assessments.

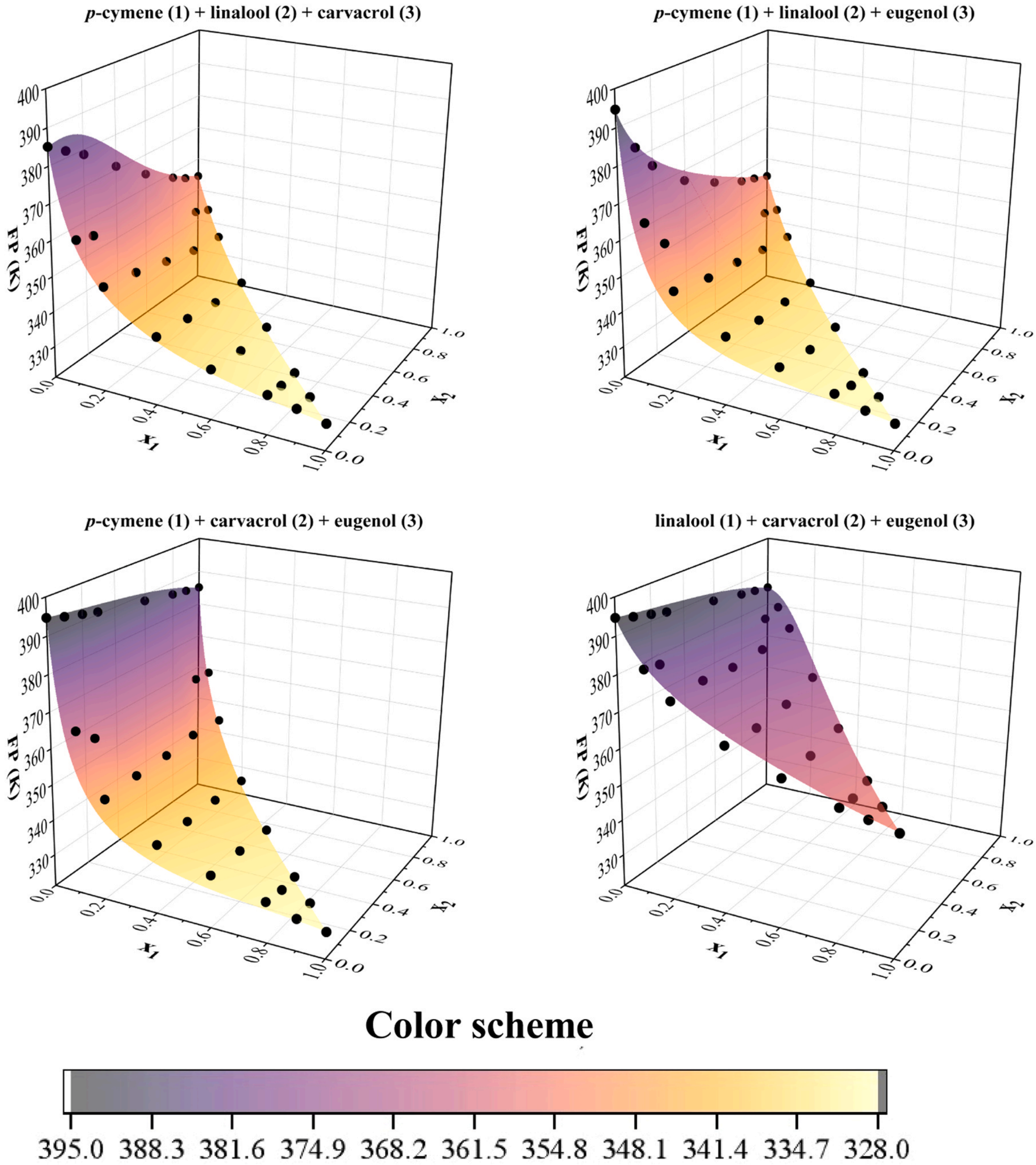

Fig. 5. Comparison of experimental FP values (●) with the profiles predicted by the Liaw-UNIFAC model for the studied ternary mixtures.

5. Conclusion

This work provides the first comprehensive investigation into the FP behavior of four monoterpenoids—*p*-cymene, linalool, carvacrol, and eugenol—and their binary and ternary mixtures. These compounds are key constituents of essential oils from sources such as cinnamon, basil, winter savory, and oregano (including Mediterranean and Mexican varieties). Experimental data were obtained using the ASTM D6450 closed-cup method for pure compounds and mixtures, and the results for the mixtures were compared with predictions from the ideal approach, the Liaw-UNIFAC model, and COSMO-RS.

The high precision of the experimental data was confirmed by the very low coefficient of variation ($\leq$ 0.34%). The FP values of the pure compounds were in excellent agreement with literature data from closed-cup-based methodologies, which are the recommended standards for volatile liquids. Despite sharing the same carbon number, the FPs of the monoterpenoids varied significantly, from 328.4 K (*p*-cymene) to 394.7 K (eugenol). Furthermore, a strong linear correlation was observed between the flash point and the normal boiling point (NBP), resulting in a simplified empirical model for preliminary FP estimates within the (420–530) K NBP range. This correlation is currently specific to the monoterpenoid family and constrained by the limited experimental FP dataset (7 data points) used for its development. Nevertheless, when benchmarked against COSMO-RS predictions, this proposed linear correlation yielded a slightly superior description of the FP data, although both approaches demonstrated comparable performance.

For the mixtures, the FP was found to decrease as the content of the more volatile component increased. A clear structure-property relationship was observed: systems containing *p*-cymene consistently exhibited FPs lower than ideal predictions, indicating dominant repulsive interactions. In contrast, the linalool + carvacrol and linalool + carvacrol + eugenol systems showed FP values above the ideal values,

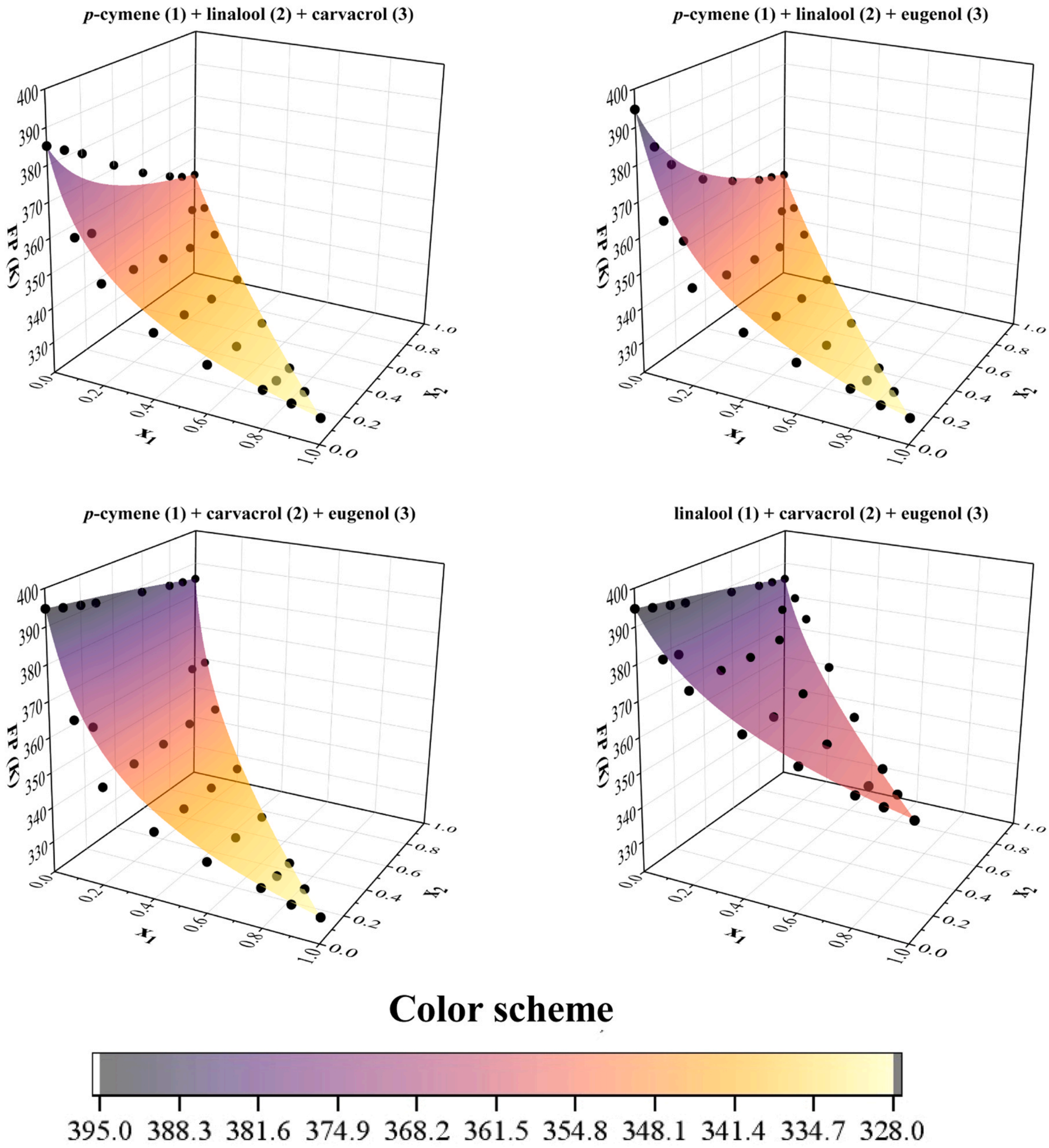

Fig. 6. Comparison of experimental FP values (●) with the profiles predicted by the ideal approach for the studied ternary mixtures.

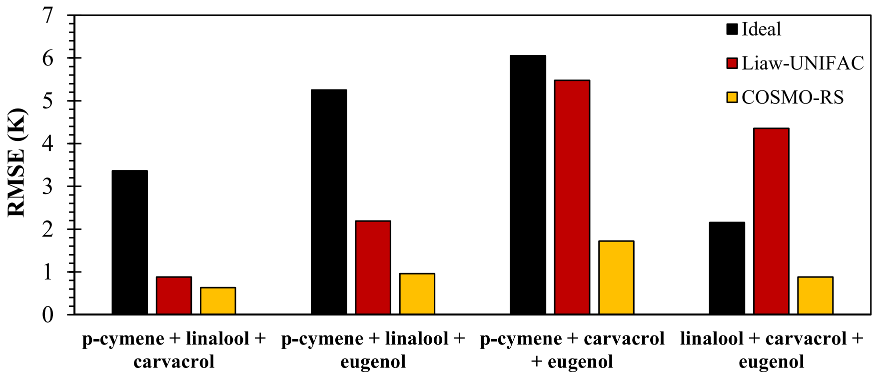

Fig. 7. Overview of the root-square mean errors (RMSE) obtained between the experimental and predicted FP values of the ternary terpene mixtures.

indicating the prevalence of attractive forces.

Among the predictive strategies, COSMO-RS delivered the best overall performance for all systems, with global RMSE values of 0.8 K and 1.0 K for the binary and ternary systems, respectively. The performance of the other tested models was system-dependent: Liaw-UNIFAC was more accurate for hydrocarbon-containing systems (except for those with eugenol), while the ideal approach surprisingly outperformed it for oxygenated mixtures, where Liaw-UNIFAC consistently overestimated attractive interactions.

Although essential oils are widely classified as flammable liquids (FP ≤ 93 °C) under the OSHA criteria, the scarcity of reliable FP data poses a challenge for robust safety assessments. This work addresses this critical knowledge gap by providing novel experimental FP data for new sets of key multicomponent terpene mixtures and by rigorously evaluating the performance of predictive models. Furthermore, from a practical standpoint, the quantum-chemistry-based COSMO-RS proved to be a robust and highly reliable tool for representing FP behavior across all tested mixtures, offering considerably improved performance for the diverse mixtures commonly found in EOs from *Origanum*, cinnamon, basil, and winter savory species (RMSE < 1 K). On the other hand, the ideal model shows reasonable performance only for mixtures containing eugenol and other oxygenated monoterpenoids, being inadequate to represent mixtures where repulsive interactions are observed. Specifically, FP overestimations of up to 10 K were observed in ternary systems containing *p*-cymene and eugenol using the ideal approach, an error that could lead to dangerous underestimations of fire hazards. The Liaw-UNIFAC offered intermediate performance between COSMO-RS and the ideal approach and is not recommended for systems containing strong intermolecular or intramolecular hydrogen bonding, as the published UNIFAC parameters fail to properly capture these specific and more complex associations.

The findings herein not only expand the available fundamental data but also reinforce a validated modeling framework to support more accurate fire hazard and risk assessment studies when processing and handling terpene-rich mixtures. Looking forward, future research should expand on the current limited knowledge of the FP of terpene multicomponent mixtures, raw essential oil matrices, and emerging terpene-based solvents. Moreover, a critical gap remains regarding the FP behavior of EO constituents mixed with common extraction solvents, such as alkanes and short-chain alcohols. Investigating such topics through combined experimental and modeling approaches will provide the key information necessary to implement effective industrial safety protocols within the growing biorefinery sector.

CRediT authorship contribution statement

Filipe Hobi Bordón Sosa: Writing – review & editing. **Débora Costa do Nascimento:** Writing – review & editing, Software. **Fernanda Sossai Altoé:** Writing – review & editing, Validation, Investigation. **Eduardo de Souza Esperança:** Writing – review & editing, Validation, Investigation. **Antonio M. Barbosa Neto:** Software, Funding acquisition. **Mariana Conceição da Costa:** Writing – review & editing, Resources, Project administration, Funding acquisition, Conceptualization. **Sérgio M. Vilas-Boas:** Writing – original draft, Visualization, Software, Methodology, Investigation, Formal analysis, Data curation, Conceptualization.

Declaration of Generative AI and AI-assisted technologies in the writing process

During the preparation of this work, the authors used Gemini 2.5 Pro exclusively to improve language and readability. After using this tool/service, the authors reviewed and edited the content as needed and take full responsibility for the content of the published article.

Declaration of Competing Interest

The authors declare that they have no known competing financial interests or personal relationships that could have appeared to influence the work reported in this paper.

Acknowledgements

This study was financed by the National Council for Scientific and Technological Development (CNPq), grants 312848/2023–4, 444231/2024–2, and 443214/2024–7, the São Paulo Research Foundation (FAPESP), grants 2021/11380–5, 2024/11984–6, 2024/01069–9, and 2025/20664–8, FAEPEX Unicamp, and partially developed within the scope of the project CICECO Aveiro Institute of Materials, UID/50011/2025 (DOI 10.54499/UID/50011/2025) & LA/P/0006/2020 (DOI 10.54499/LA/P/0006/2020), financed by national funds through the FCT/MCTES (PIDDAC). Sérgio M. Vilas-Boas would like to thank the Ministry of Science, Innovation and Universities of Spain for the support through the Juan de la Cierva grant (JDC2023–051385-I). Filipe H. B. Sosa acknowledges FCT – Fundação para a Ciência e a Tecnologia, I.P. for the researcher contract CEECIND/07209/2022 (https://doi.org/10.54499/2022.07209.CEECIND/CP1720/CT0019) under the Scientific Employment Stimulus Individual Call 2022.

Description of supplementary material

The Supplementary Material includes the following: regressed Antoine constants used in the FP calculations with the Liaw-UNIFAC and ideal models; a comparison between the pure terpene FP values estimated using the proposed linear FP-NBP correlation with those predicted with the COSMO-RS model; and Root-Mean-Square Errors (RMSE) values comparing the experimental and predicted FP values for the binary and ternary mixtures.

Appendix A. Supporting information

Supplementary data associated with this article can be found in the online version at doi:10.1016/j.psep.2026.108687.

References

Al-Maqtari, Q.A., Rehman, A., Mahdi, A.A., Al-Ansi, W., Wei, M., Yanyu, Z., Phyo, H.M., Galeboe, O., Yao, W., 2022. Application of essential oils as preservatives in food systems: challenges and future prospectives – a review. Phytochem. Rev. 21, 1209–1246.

Api, A.M., Belsito, D., Bhatia, S.P., Bruze, M., Calow, P., Dagli, M.L., Dekant, W., Fryer, A. D., Kromidas, L., La Cava, S., Lalko, J.F., Lapczynski, A., Liebler, D.C., Miyachi, Y., Politano, V.T., Ritacco, G., Salvito, D., Shen, J., Schultz, T.W., Sipes, I.G., Wall, B., Wilcox, D.K., 2015. RIFM fragrance ingredient safety assessment, Linalool, CAS registry number 78-70-6. Food Chem. Toxicol. 82, S29–S38.

Banihashemi, M., Movagharnejad, K., 2018. Use of group contribution method and intelligent algorithms to predict the flash temperature of binary mixtures. Process Saf. Environ. Prot. 117, 539–550.

Baser, K.H., Bonello, J.M., 2025. Global trade of essential oils. J. Essent. Oil Res. 37, 208–214.

2021 BIOVIA COSMOconf 21, 2021.

Baycheva, S.K., Dobreva, K.Z., 2021. Chemical composition of Bulgarian white oregano (Origanum heracleoticum L.) essential oils. IOP Conf. Ser. Mater. Sci. Eng. 1031, 012107.

BIOVIA COSMOtherm, 2021. Release 2021, Dassault Systèmes.

BIOVIA COSMOtherm 2020, 2020. Reference manual.

Campbell, J.R., Luthy, R.G., 1985. Prediction of aromatic solute partition coefficients using the UNIFAC group contribution model. Environ. Sci. Technol. 19, 980–985.

Capdevila, S., Grau, D., Cristóbal, R., Moré, E., De las Heras, X., 2025. Chemical composition of wild populations of Thymus vulgaris and Satureja montana in central Catalonia, Spain. JSFA Rep. 5, 234–246.

Carroll, F.A., Lin, C.-Y., Quina, F.H., 2011. Simple method to evaluate and to predict flash points of organic compounds. Ind. Eng. Chem. Res. 50, 4796–4800.

Carvalho, I.T., Estevinho, B.N., Santos, L., 2016. Application of microencapsulated essential oils in cosmetic and personal healthcare products - A review. Int. J. Cosmet. Sci. 38, 109–119.

Chericoni, S., Prieto, J.M., Iacopini, P., Cioni, P., Morelli, I., 2005. vitro activity of the essential oil of Cinnamomum zeylanicum and eugenol in peroxynitrite-induced oxidative processes. J. Agric. Food Chem. 53, 4762–4765.

Cho, S.-M., Kim, J.-H., Kim, S.-H., Park, S.-Y., Kim, J.-C., Choi, I.-G., 2018. A comparative study on the fuel properties of biodiesel from woody essential oil depending on terpene composition. Fuel 218, 375–384.

Cimino, C., Maurel, O.M., Musumeci, T., Bonaccorso, A., Drago, F., Souto, E.M.B., Pignatello, R., Carbone, C., 2021. Essential oils: pharmaceutical applications and encapsulation strategies into lipid-based delivery systems. Pharmaceutics 13, 327.

Clará, R.A., Marigliano, A.C.G., Sólimo, H.N., 2009. Density, viscosity, and refractive index in the range (283.15–353.15) K and vapor pressure of α-pinene, d-limonene, (±)-linalool, and citral over the pressure range 1.0 kPa atmospheric pressure. J. Chem. Eng. Data 54, 1087–1090.

Clark, G.S., 1988. A profile: An aroma chemical linalool. Perfum. Flav 8–9, 49–54.

Cornell, J.A., 2002. Experiments with Mixtures. Wiley Series in Probability and Statistics. Wiley.

Costa do Nascimento, D., Dorighello Carareto, N.D., Marinho Barbosa Neto, A., Gerbaud, V., da Costa, M.C., 2020. Flash point prediction with UNIFAC type models of ethylic biodiesel and binary/ternary mixtures of FAEEs. Fuel 281, 118717.

Costa do Nascimento, D., Conti, D.C., Barbosa Neto, A.M., Costa, M.C., 2021. Flash point measurement and prediction of dodecane + ethanol + FAEE systems. Fuel 306, 121723.

Costa do Nascimento, D., Souza, M.P., de, O., Hentges, L., de, O., Dias, R.M., Marinho Barbosa Neto, A., Costa, M.C. da, 2024. Mixture flash point calculation: Recent advances and a closer look at biodiesel. ACS. Chem. Health & Saf. 31, 22–43.

Crowl, D.A., Louvar, J.F., 2011. Third ed. ed. Chemical process safety: Fundamentals with applications. Prentice Hall PTR.

De Las Heras López, I., Díaz Magdaleno, J., Dufour, J., Coto, B., 2023. Solid–liquid equilibria of binary mixtures of alcohols and aromatic hydrocarbons: experimental methods and modeling analysis. J. Therm. Anal. Calor. 148, 7217–7231.

De Liso, B.A., Pio, G., Salzano, E., 2024. Fire behaviour of liquid solvents for energy storage applications. Process Saf. Environ. Prot. 188, 726–734.

Deng, D., Li, H., Han, S., 2002. Isobaric (vapour + liquid) equilibria of (linalool + 1–propanol) and (linalool + 1–butanol). J. Chem. Thermodyn. 34, 1431–1437.

Di Benedetto, A., Sanchirico, R., Di Sarli, V., 2018. Effect of pressure on the flash point of various fuels and their binary mixtures. Process Saf. Environ. Prot. 116, 615–620.

Dias, R.M., Aquino, R.T., Krähenbühl, M.A., Costa, M.C., 2019. Flash point of fatty acid methyl ester binary mixtures. J. Chem. Eng. Data 64, 3465–3472.

Dortmund Data Bank [WWW Document], 2025. URL ⟨https://www.ddbst.com/published-parameters-unifac.html⟩ (accessed 11.24.25).

Dupeux, T., Gaudin, T., Marteau-Roussy, C., Aubry, J., Nardello-Rataj, V., 2022. COSMO-RS as an effective tool for predicting the physicochemical properties of fragrance raw materials. Flavour Fragr. J. 37, 106–120.

Eckert, F., Klamt, A., 2002. Fast solvent screening via quantum chemistry: COSMO-RS approach. AIChE J. 48, 369–385.

Fredenslund, A., Jones, R.L., Prausnitz, J.M., 1975. Group-contribution estimation of activity coefficients in nonideal liquid mixtures. AIChE J. 21, 1086–1099.

Guerrero, F., Carmona, C., Hernández, C., Toledo, M., Arriagada, A., Espinoza, L., Bergmann, J., Taborga, L., Yañez, K., Carrasco, Y., Muñoz, A.A., 2022. Drivers of flammability of Eucalyptus globulus labill Leaves: Terpenes, essential oils, and moisture content. Forests 13, 908.

Guimarães, L.H., dos, S., Chemelo, G.P., Alves, A.C.B.A., Pinheiro, J., de, J.V., Kataoka, M.S. da S., Silva, S.G., Santana de Oliveira, M., Helena de Aguiar Andrade, E., Ribeiro, A.F., Menezes, T.O. de A., 2021. Chemical composition and cytotoxicity evaluation of Lippia origanoides Kunth (Verbenaceae) leaves essential oil on human gingival fibroblasts. J. Essent. OilBear. Plants 24, 704–713.

Haghtalab, A., Seyf, J.Y., Mansouri, Y., 2016. Flash point prediction of the binary and ternary systems using the different local composition activity coefficient models. Fluid Phase Equilib. 415, 58–63.

Hanif, M.A., Nisar, S., Khan, G.S., Mushtaq, Z., Zubair, M., 2019. Essential Oils. In: Essential Oil Research. Springer International Publishing, Cham, pp. 3–17.

Henriques, J.D., de, O., Sosa, F.H.B., Dias, R.M., Martinez, P.F.M., da Costa, M.C., 2020. Flash point and excess molar volumes of binary mixtures containing d-limonene and alcohol compounds from propanol to dodecanol. J. Chem. Thermodyn. 150, 106224.

Hshieh, T.T., Hshieh, F.-Y., 2005. Closed-cup flash points and flammability properties of selected chemical compounds. J. Fire Sci. 23, 157–171.

Huo, X., Lu, Q., Wang, J., 2022. Liaw-UNIFAC flash point model for alcohols-kerosene/diesel fuel blends using average fuel structure. Process Saf. Environ. Prot. 160, 400–410.

Ilić, A.S., Antić, M.P., Jelačić, S.C., Šolević Knudsen, T.M., 2018. Chemical composition of the essential oils of three Ocimum basilicum L. Cultivars from Serbia. Not. Bot. Horti Agrobot. Cluj. Napoca 47, 347–351.

Ivanova, S., Gvozdeva, Y., Staynova, R., Grekova-Kafalova, D., Nalbantova, V., Benbassat, N., Koleva, N., Ivanov, K., 2025. Essential oils – a review of the natural evolution of applications and some future perspectives. Pharmacia 72, 1–12.

Jalaei Salmani, H., Lotfollahi, M.N., Mazloumi, S.H., 2018. A model for predicting flash point of alkane-alkane and water-alcohol mixtures by the Cubic-Plus-Association Equation of State. Process Saf. Environ. Prot. 119, 191–197.

Jávega-Cometto, M., Naranjo-Viteri, A.J., Champarini, L.G., Hereñú, C.B., Crespo, R., 2025. Plant-derived monoterpene therapies in Parkinson's Disease models: Systematic review and meta-analysis. Plants.

Klamt, A., 1995. Conductor-like screening model for real solvents: A new approach to the quantitative calculation of solvation phenomena. J. Phys. Chem. 99, 2224–2235.

Klamt, A., 2005. COSMO-RS: From quantum chemistry to fluid phase thermodynamics and drug design (ed). Computer Aided Chemical Engineering, 1st ed. Elsevier Science.

Klamt, A., 2011. The COSMO and COSMO-RS solvation models. WIREs Comput. Mol. Sci. 1, 699–709.

Klamt, A., Eckert, F., 2000. COSMO-RS: a novel and efficient method for the a priori prediction of thermophysical data of liquids. Fluid Phase Equilib. 172, 43–72.

Klamt, A., Jonas, V., Bürger, T., Lohrenz, J.C.W., 1998. Refinement and parametrization of COSMO-RS. J. Phys. Chem. A 102, 5074–5085.

Klamt, A., Eckert, F., Arlt, W., 2010. COSMO-RS: an alternative to simulation for calculating thermodynamic properties of liquid mixtures. Annu. Rev. Chem. Biomol. Eng. 1, 101–122.

Klamt, A., Schwöbel, J., Huniar, U., Koch, L., Terzi, S., Gaudin, T., 2019. COSMO: Plex: self-consistent simulation of self-organizing inhomogeneous systems based on COSMO-RS. Phys. Chem. Chem. Phys. 21, 9225–9238.

Kobe, K.A., Okabe, T.S., Ramstad, M.T., Huemmer, P.M., 1941. P-cymene studies. VI. Vapor pressure of p-cymene, some of its derivatives and related compounds. J. Am. Chem. Soc. 63, 3251–3252.

Kontogeorgis, G.M., Folas, G.K., 2010. Thermodynamic models for industrial applications. Wiley.

Kordali, S., Cakir, A., Ozer, H., Cakmakci, R., Kesdek, M., Mete, E., 2008. Antifungal, phytotoxic and insecticidal properties of essential oil isolated from Turkish Origanum acutidens and its three components, carvacrol, thymol and p-cymene. Bioresour. Technol. 99, 8788–8795.

Lakzian, K., Liaw, H., 2021. Flash point investigation of ternary mixtures of 1-butanol/2-pentanol + acetic acid + ethylbenzene. Process Saf. Environ. Prot. 154, 131–141.

Lakzian, K., Liaw, H.-J., 2024. Flash point and safety evaluation of binary mixture of diphenyl ether + biphenyl: A commonly utilized heat transfer fluid. Thermochim. Acta 733, 179673.

Lapuerta, M., Tobío-Pérez, I., Ortiz-Alvarez, M., Donoso, D., Canoira, L., Piloto-Rodríguez, R., 2023. Heterogeneous catalytic conversion of terpenes into biofuels: An open pathway to sustainable fuels. Energ. (Basel) 16, 2526.

Le, T.C., Ballard, M., Casey, P., Liu, M.S., Winkler, D.A., 2015. Illuminating flasmh point: Comprehensive prediction models. Mol. Inf. 34, 18–27.

Lecat, M., 1927. Nouveaux azeotropes binaires: Cinquième liste. Recl. Des. Trav. Chim. Des. PaysBas 46, 240–247.

Lecat, M., 1928. Nouveaux azeotropes binaires: Huitième liste. Recl. Des. Trav. Chim. Des. PaysBas 47, 13–18.

Li, X., Duan, P.P., Sun, K.N., Yan, X., 2014. Prediction of the flash point of binary and ternary straight-chain alkane mixtures. Adv. Mater. Sci. Eng. 2014, 1–5.

Liaw, H.-J., Tang, Q.-R., 2025. Flash point prediction of binary mixtures of ionic liquid and flammable solvent. J. Loss Prev. Process Ind. 96, 105631.

Liaw, H.-J., Yang, C.-A., 2020. Maximum flash point behavior of ternary mixtures with single and two maximum flash point binary constituents. Process Saf. Environ. Prot. 143, 293–303.

Liaw, H.-J., Lee, Y.-H., Tang, C.-L., Hsu, H.-H., Liu, J.-H., 2002. A mathematical model for predicting the flash point of binary solutions. J. Loss Prev. Process Ind. 15, 429–438.

Liaw, H.-J., Tang, C.-L., Lai, J.-S., 2004. A model for predicting the flash point of ternary flammable solutions of liquid. Combust. Flame 138, 308–319.

Liaw, H.-J., Gerbaud, V., Li, Y.-H., 2011. Prediction of miscible mixtures flash-point from UNIFAC group contribution methods. Fluid Phase Equilib. 300, 70–82.

Liaw, H.-J., Hsu, W.-C., Lakzian, K., 2022. Exploration of two types of maximum–minimum flash point behavior of ternary mixtures. J. Loss Prev. Process Ind. 80, 104915.

Lin, S.-T., Chang, J., Wang, S., Goddard, W.A., Sandler, S.I., 2004. Prediction of vapor pressures and enthalpies of vaporization using a COSMO solvation model. J. Phys. Chem. A 108, 7429–7439.

Linder, E.G., 1931. Vapor pressures of some hydrocarbons. J. Phys. Chem. 35, 531–535.

Lindokuhle, M., Tumba, K., Nkosi, N., Ngema, T., 2026. Terpene-based hydrophobic (D) ESs: A systematic review of physiochemical properties. Chem. Thermodyn. Therm. Anal. 21, 100249.

Lorenzo-Llanes, J., Palomar, J., Escalona, N., Canales, R.I., 2025. COSMO-RS-based solvent screening and experimental analysis for recovering added-value chemicals from the bio-oil aqueous phase. Sep. Purif. Technol. 369, 133104.

Luning Prak, D.J., Luning Prak, P.J., Cowart, J.S., Trulove, P.C., 2017. Densities and viscosities at 293.15–373.15 K, speeds of sound and bulk moduli at 293.15–333.15 K, surface tensions, and flash points of binary mixtures of n -hexadecane and alkylbenzenes at 0.1 MPa. J. Chem. Eng. Data 62, 1673–1688.

Masyita, A., Mustika Sari, R., Dwi Astuti, A., Yasir, B., Rahma Rumata, N., Emran, T.Bin, Nainu, F., Simal-Gandara, J., 2022. Terpenes and terpenoids as main bioactive compounds of essential oils, their roles in human health and potential application as natural food preservatives. Food Chem. X 13, 100217.

Mcdonald, R.A., Shrader, S.A., Stull, D.R., 1959. Vapor pressures and freezing points of 30 organics. J. Chem. Eng. Data 4, 311–313.

Milos, M., Radonic, A., Bezic, N., Dunkic, V., 2001. Localities and seasonal variations in the chemical composition of essential oils of Satureja montana L. and S. cuneifolia Ten. Flavour Fragr. J. 16, 157–160.

Mukhtar Gunam Resul, M.F., Rehman, A., Saleem, F., Usman, M., López Fernández, A.M., Eze, V.C., Harvey, A.P., 2023. Recent advances in catalytic and non-catalytic epoxidation of terpenes: a pathway to bio-based polymers from waste biomass. RSC Adv. 13, 32940–32971.

Muráriková, A., Ťažký, A., Neugebauerová, J., Planková, A., Jampílek, J., Mučaji, P., Mikuš, P., 2017. Characterization of essential oil composition in different basil species and pot cultures by a GC-MS method. Molecules 22, 1221.

Nazari, B., Keshavarz, M.H., Hassanzadeh, A., 2019. Reliable prediction of the flash point of organic compounds containing hazardous peroxide functional groups as compared to the best available methods. Process Saf. Environ. Prot. 132, 134–141.

Occupational Safety & Health Administration [OSHA], 2012. Standards CFR 1910.106.

Olbert-Majkut, A., Wierzejewska, M., 2008. Conformational study of eugenol by density functional theory method and matrix-isolation infrared spectroscopy. J. Phys. Chem. A 112, 5691–5699.

Ozturk, B., Gonzalez-Miquel, M., 2019. Alkanediol-based deep eutectic solvents for isolation of terpenoids from citrus essential oil: Experimental evaluation and COSMO-RS studies. Sep. Purif. Technol. 227, 1–9.

Patil, G.S., 1988. Estimation of flash point. Fire Mater. 12, 127–131.

Paulino, B.N., Silva, G.N.S., Araújo, F.F., Néri-Numa, I.A., Pastore, G.M., Bicas, J.L., Molina, G., 2022. Beyond natural aromas: The bioactive and technological potential of monoterpenes. Trends Food Sci. Technol. 128, 188–201.

Perry, R.E., Thodos, G., 1952. Vapor pressures of the light normal saturated hydrocarbons. Ind. Eng. Chem. 44, 1649–1653.

Phoon, L.Y., Mustaffa, A.A., Hashim, H., Mat, R., 2014. A review of flash point prediction models for flammable liquid mixtures. Ind. Eng. Chem. Res. 53, 12553–12565.

Poling, B.E., Prausnitz, J.M., O'Connel, J.P., 2001. The properties of gases and liquids, 5th ed, Experimental Thermal and Fluid Science. McGraw-Hill.

Prausnitz, J.M., Lichtenthaler, R.N., Azevedo, E.G. de, 1999. Molecular thermodynamics of fluid-phase equilibria, 3rd ed. ed. Pretnice Hall PTR.

Qin, Y., Chen, X., Wang, L., Wei, Xiaojie, Mo, H., Wei, Xuejuan, Liang, J., 2022. Measurement and correlation of isothermal vapor-liquid equilibrium for (−)-β-caryophyllene + p-cymene with dehydroabietic acid at 313.15, 323.15, and 333.15K. J. Taiwan Inst. Chem. Eng. 138, 104466.

Rahman, S.M.A., Van, T.C., Hossain, F.M., Jafari, M., Dowell, A., Islam, M.A., Nabi, M.N., Marchese, A.J., Tryner, J., Rainey, T., Ristovski, Z.D., Brown, R.J., 2019. Fuel properties and emission characteristics of essential oil blends in a compression ignition engine. Fuel 238, 440–453.

Raina, V.K., Srivastava, S.K., Aggarwal, K.K., Ramesh, S., Kumar, S., 2001. Essential oil composition of Cinnamomum zeylanicum Blume leaves from Little Andaman, India. Flavour Fragr. J. 16, 374–376.

Reinisch, J., Klamt, A., 2015. Predicting flash points of pure compounds and mixtures with COSMO-RS. Ind. Eng. Chem. Res. 54, 12974–12980.

Rodrigues, V.H.S., Almeida, R.N., Vargas, R.M.F., Cassel, E., 2022. Vapor pressure and vapor-liquid equilibrium data for eugenol/caryophyllene binary system at low pressures by experimental and predictive methods. J. Chem. Thermodyn. 168, 106725.

Rowley, J.R., Freeman, D.K., Rowley, R.L., Oscarson, J.L., Giles, N.F., Wilding, W.V., 2010. Flash point: Evaluation, experimentation and estimation. Int. J. Thermophys. 31, 875–887.

Russo, A.Y., Konnova, M.E., Andreeva, I.V., Verevkin, S.P., 2019. Vaporization thermodynamics of compounds modeling lignin structural units. Fluid Phase Equilib. 491, 45–55.

Sánchez-Velandia, J.E., Gallego-Villada, L.A., Mäki-Arvela, P., Sidorenko, A., Yu. Murzin, D., 2025. Upgrading biomass to high-added value chemicals: synthesis of monoterpenes-based compounds using catalytic green chemical pathways. Catal. Rev. 67, 371–496.

Schmidt, E., Jirovetz, L., Buchbauer, G., Eller, G.A., Stoilova, I., Krastanov, A., Stoyanova, A., Geissler, M., 2006. Composition and antioxidant activities of the essential oil of cinnamon (Cinnamomum zeylanicum Blume) leaves from Sri Lanka. J. Essent. Oil Bear. Plants 9, 170–182.

Sharmeen, J.B., Mahomoodally, F.M., Zengin, G., Maggi, F., 2021. Essential oils as natural sources of fragrance compounds for cosmetics and cosmeceuticals. Molecules 26, 666.

Shen, Y., Zhao, H., Sheng, X., 2023. Theoretical study of hydrogen bond interactions of methanesulfonic acid with eugenol/methyleugenol. Comput. Theor. Chem. 1219, 113977.

Sigma-Aldrich, 2022. Linalool Safety Data Sheet.

Sigma-Aldrich, 2023. Eugenol Safety Data Sheet.

Sigma-Aldrich, 2024. p-Cymene Safety Data Sheet.

da Silva, A.T., Cândido, A.E.C.M., Júnior, E., do, C.M., do, É., Moura, G.N., Souza, M.P.S., de, R., Guimarães, F.S., Peixoto, M.L., de, R., de Oliveira, M., da Costa, M.M, H.P., 2024. Bactericidal and synergistic effects of Lippia origanoides essential oil and its main constituents against multidrug-resistant strains of Acinetobacter baumannii. ACS Omega 9, 43927–43939.

Sosa, F.H.B., Temoteo, F.A., Dias, R.M., Costa do Nascimento, D., Neto, A.M.B., da Costa, M.C., 2024. Flash point of binary and ternary mixture of biojet blends: Experimental data and modeling. Fluid Phase Equilib. 576, 113940.

Stanojevic, L.P., Stanojevic, J.S., Savic, V.Lj, Cvetkovic, D.J., Kolarevic, A., Marjanovic-Balaban, Z., Nikolic, L.B., 2019. Peppermint and basil essential oils: Chemical composition, in vitro antioxidant activity and in vivo estimation of skin irritation. J. Essent. Oil Bear. Plants 5026, 1–15.

Steffen, C., Thomas, K., Huniar, U., Hellweg, A., Rubner, O., Schroer, A., 2010. Software news and updates TmoleX — A graphical user interface for TURBOMOLE. J. Comput. Chem. 31, 2967–2970.

Štejfa, V., Fulem, M., Růžička, K., 2023. Thermodynamic study of selected aromatic monoterpenoids. J. Mol. Liq. 380, 121724.

Stull, D.R., 1947. Pressure of pure substances. Oragnic compounds. Ind. Eng. Chem. 39, 518–536.

Sun, Y., Chen, Q., Guo, J., Adumene, S., Goleiji, E., Yazdi, M., 2025. A risk-based review of dangerous goods storage and handling at a manufacturing facility. Int. J. Adv. Manuf. Technol. 138, 4313–4336.

Teixeira, G., Abranches, D.O., Silva, L.P., Vilas-Boas, S.M., Pinho, S.P., Ferreira, A.I.M.C. L., Santos, L.M.N.B.F., Ferreira, O., Coutinho, J.A.P., 2022. Liquefying flavonoids with terpenoids through deep eutectic solvent formation. Molecules 27, 2649.

ThermoFisher Scientific, 2022. Carvacrol Safety Data Sheet.

Torabian, E., Sobati, M.A., 2017. New models for predicting the flash point of mixtures containing different alcohols. Process Saf. Environ. Prot. 111, 439–448.

Uc-Cachón, A.H., Calvo-Irabien, L.M., Dzul-Beh, A. de J., Dzib-Baak, H.E., Grijalva-Arango, R., Molina-Salinas, G.M., 2024. Potential anti-infectious activity of essential oil chemotypes of Lippia origanoides Kunth on antibiotic-resistant Staphylococcus aureus strains. Plants 13, 1172.

University of Hertfordshire, 2025. EU BPDB: Biopesticides DataBase - Eugenol [WWW Document]. URL ⟨https://sitem.herts.ac.uk/aeru/bpdb/Reports/2008.htm⟩ (accessed 7.27.25).

Vidal, M., Rogers, W.J., Mannan, M.S., 2006. Prediction of minimum flash point behaviour for binary mixtures. Process Saf. Environ. Prot. 84, 1–9.

Vilas-Boas, S.M., Pokorný, V., Štejfa, V., Ferreira, O., Pinho, S.P., Růžička, K., Fulem, M., 2019. Vapor pressure and thermophysical properties of eugenol and (+)-carvone. Fluid Phase Equilib. 499, 112248.

Vilas-Boas, S.M., do Nascimento, D.C., Dias, R.M., Rozo, G.H., Barbosa Neto, A.M., Ferreira, O., Pinho, S.P., da Costa, M.C., 2023. Flash point of binary and ternary monoterpene mixtures: Experimental and modeling. Process Saf. Environ. Prot. 172, 1048–1057.

Vilas-Boas, S.M., da Costa, M.C., Coutinho, J.A.P., Ferreira, O., Pinho, S.P., 2022. Octanol–water partition coefficients and aqueous solubility data of monoterpenoids: Experimental, modeling, and environmental distribution. Ind. Eng. Chem. Res. 61, 3154–3167.

Vilas-Boas, S.M., Coelho, A.Z., Martins, M.A.R., Coutinho, J.A.P., Ferreira, O., Pinho, S. P., 2023a. Evaluation of ionic liquids for the sustainable fractionation of essential oils. Ind. Eng. Chem. Res. 62, 6749–6758.

Vilas-Boas, S.M., Cordova, I.W., Abranches, D.O., Coutinho, J.A.P., Ferreira, O., Pinho, S. P., 2023b. Modeling the solubility of monoterpenoids with hybrid and predictive thermodynamic tools. Ind. Eng. Chem. Res. 62, 5326–5335.

Vilas-Boas, S.M., Coutinho, J.A., Pinho, S.P., Ferreira, O., 2025. Solvent screening for the purification of monoterpenoids by countercurrent and centrifugal partition chromatography. J. Chem. Technol. & Biotechnol. 100, 166–175.

Yu, J., 2025. Chemical composition of essential oils and their potential applications in postharvest storage of cereal grains. Molecules.

Yuwono, M., Siswandono, Hafid, A.F., Poernomo, A.T., Agil, M., Indrayanto, G., Ebel, S., 2002. Eugenol. Anal. Profiles Drug Subst. Excip. 29, 149–177.

Zaitsau, D.H., Verevkin, S.P., Sazonova, A.Y., 2015. Vapor pressures and vaporization enthalpies of 5-nonanone, linalool and 6-methyl-5-hepten-2-one. Data evaluation. Fluid Phase Equilib. 386, 140–148.

Zambom, A., Vilas-Boas, S.M., Silva, L.P., Martins, M.A.R., Ferreira, O., Pinho, S., 2023. The role of the anion in imidazolium-based ionic liquids for fuel and terpenes processing. Molecules 28, 2456.

Zhang, W., Wang, X., Jiang, Z., Zhao, Y., Li, Y., 2025. Separation of biomass furans by terpenoid-based hydrophobic deep eutectic solvents probed by molecular dynamics simulations and liquid-liquid extraction experiments. Process Saf. Environ. Prot. 193, 1080–1093.

Zielińska-Błajet, M., Feder-Kubis, J., 2020. Monoterpenes and their derivatives—recent development in biological and medical applications. Int. J. Mol. Sci. 21, 1–38.

Zuzarte, M., Sousa, C., Alves-Silva, J., Salgueiro, L., 2024. Plant monoterpenes and essential oils as potential anti-ageing agents: insights from preclinical data. Biomedicines 12, 365.